Chapter 2

Role of Plasma Catalysis in the Microwave Plasma-Assisted Conversion of CO_2

Guoxing Chen, Nikolay Britun, Thomas Godfroid, Marie-Paule Delplancke-Ogletree and Rony Snyders

Additional information is available at the end of the chapter

http://dx.doi.org/10.5772/67874

Abstract

Climate change and global warming caused by the increasing emissions of greenhouse gases (such as CO_2) recently attract attention of the scientific community. The combination of plasma and catalysis is of great interest for turning plasma chemistry in applications related to pollution and energy issues. In this chapter, our recent research efforts related to optimization of the conversion of CO_2 and CO_2/H_2O mixtures in a pulsed surface-wave sustained microwave discharge are presented. The effects of different plasma operating conditions and catalyst preparation methods on the CO_2 conversion and its energy efficiency are discussed. It is demonstrated that, compared to the plasma-only case, the CO_2 conversion and energy efficiency can be enhanced by a factor of ~2.1 by selecting the appropriate conditions. The catalyst characterization shows that Ar plasma treatment results in a higher density of oxygen vacancies and a comparatively uniform distribution of NiO on the TiO_2 surface, which strongly influence CO_2 conversion and energy efficiencies of this process. The dissociative electron attachment of CO_2 at the catalyst surface enhanced by the oxygen vacancies and plasma electrons may explain the increase of conversion and energy efficiencies in this case. A mechanism of plasma-catalytic conversion of CO_2 at the catalyst surface in CO_2 and CO_2/H_2O mixtures is proposed.

Keywords: green energy, CO_2 conversion, plasma catalysis, microwave discharge, NiO/TiO_2 catalyst

1. Introduction

One of the biggest concerns of the twenty-first century is the effect of global warming and its destructive consequences on the global ecosystem. Evidence indicated that the main cause of increased amounts of greenhouse gas emissions (such as CO_2) are the human activities related to the industrialization and burning of the fossil fuels. The process of conversion of CO_2 along with the other greenhouse gases into value-added chemicals or new fuels has attracted considerable attention because of the current background of fossil resources depletion and increase of CO_2 emissions. If a renewable (from sunlight or wind) or nuclear energy source drives the dissociation of CO_2 or other greenhouse gases, the renewable or nuclear energy can be stored as chemical energy in fuels. In this context, CO_2 reutilization to synthesize syngas, valuable fuels, or chemical compounds as well as pure CO_2 dissociation into CO and O_2 is of a special interest. Large efforts have been made to develop energy-efficient technologies [1–7].

Different techniques for conversion of CO_2 into value-added chemical compounds or fuels activated by heat or electricity have been developed and studied, namely thermolysis, photocatalysis, and electrochemical methods [1–5]. The CO_2 thermal splitting is thermodynamically and energetically favorable only at very high temperatures (1400–1800°C) and the conversion efficiency is very low. A prototype of CO_2 thermolysis chamber using only solar energy was developed by Traynor and Jensen [2]. The measured net conversion of CO_2 to CO was close to 6% under optimal conditions. The maximum conversion of solar to chemical energy was 5%. Recently, photocatalytic conversion of CO_2 using solar energy has attracted more and more attention. However, one of the greatest drawbacks is the low conversion efficiency at present. Moreover, its application is limited due to the numerous disadvantages [3, 4]: (1) inefficient reactor system, (2) catalyst activation needing long periods of irradiation, and (3) inefficient exploitation of visible light. High-temperature electrolysis is another promising method since it can effectively convert the electrical energy into chemical energy (78–87%) [5]. Electrolysis of CO_2 in the liquid phase has been investigated extensively while only few studies have been reported for electrolysis of CO_2 in the gas phase. Much effort should be made to overcome the drawbacks such as short-term stability of electrolytes, using expensive or scarce materials, and whole system heating.

Plasma technology represents an alternative approach to the above-mentioned methods. The nonthermal plasma technology is considered to be an attractive alternative to other (classical) technologies for converting inert carbon emissions (such as CO_2) into valuable fuels and chemicals, due to its nonequilibrium characteristics, environmental-safety, scalability, and low power requirements [6]. The fundamental properties and usefulness of the nonthermal plasmas for conversion of carbon dioxide as well as for related plasma technologies are extensively reviewed by Fridman [6], Zou and Liu [7], and by the other numerous authors. Nonthermal plasmas including dielectric barrier discharges (DBDs) [8–13], microwave discharges (MWs) [14–21], gliding arc plasmatrons (GAPs) [22–24], glow discharges [25], radio frequency (RF) discharges [26], and corona discharge [27] have been investigated for CO_2 conversion so far. However, a known trade-off between the energy efficiency and conversion efficiency is observed in plasma-assisted dissociation of pure CO_2. In order to overcome this trade-off, a plasma-assisted catalytic process with plasma activation of the catalysts to

http://dx.doi.org/10.5772/67874

increase the conversion efficiency while maintaining high energy efficiency has been proposed. The combination of heterogeneous catalysis and plasma activation, known as plasma catalysis, has attracted increasing interest [28–31]. Plasma-catalytic conversion of CO_2 is a complex and challenging process involving a large number of physical and chemical reactions. The efficiency of this process can be controlled by means of the plasma parameters themselves, as well as by the catalyst properties. This suggests that more systematic studies on both the plasma effects and the chemical effects of the catalyst are necessary.

It is well known that the vibrational excitation is considered to be the most efficient elementary process in CO_2 plasmas to stimulate the endothermic CO_2 decomposition via the so-called vibrational ladder climbing process [6]. Due to its high degree of nonequilibrium, microwave plasma excites highly vibrational states of CO_2 molecules, which are energy-efficient for CO_2 decomposition. In this regard, combining catalysis with microwave plasmas could be especially promising, as the catalyst surface can reach a somewhat elevated temperature and possibly induce a synergy. Up to now, there are only a limited number of attempts for combining catalyst with microwave plasma [15, 17, 19–21].

The present Chapter critically summarizes the plasma-catalyst phenomena for optimization of the microwave plasma-assisted CO_2 conversion focusing on NiO/TiO_2 catalysts. It is focused on the investigation of several plasma-catalytic effects and their influences including the catalyst preparation methods, plasma activation and NiO content, aiming at enhancing our understanding of the plasma-catalytic CO_2 conversion process.

2. Brief theoretical background

The excitation of both CO{_2} and water vapor is required for effective dissociation. The high energy plasma electrons have the ability to efficiently excite and dissociate CO_2 and H_2O via collisional processes. The dissociation of a CO_2 molecule is represented by the following global reaction [6]:

$$CO_2 \rightarrow CO + \frac{1}{2}O_2,\ \Delta H = 2.9\,\text{eV/molecule} \tag{1}$$

The process given by Eq.1 can be represented by an electron impact CO_2 dissociation [6]:

$$CO_2 \rightarrow CO + O,\ \Delta H = 5.5\,\text{eV/molecule} \tag{1a}$$

following either by O recombination into O_2 [Eq. (1b)] or by the reaction with a ground state (but vibrationally excited) CO_2 molecule [Eq. (1c)]:

$$M + O + O \rightarrow O_2 + M\,(\text{M is a particle}) \tag{1b}$$

$$O + CO_2 \rightarrow CO + O_2,\ \Delta H = 0.3\,\text{eV/molecule}. \tag{1c}$$

Besides this, CO can be easily converted into CO_2 with the production of H_2 in the presence of water, which is known as the water-gas shift reaction (WGSR):

$$CO + H_2O \rightleftarrows CO_2 + H_2,\ \Delta H = -0.4\,\text{eV/molecule (forward direction)}. \tag{2}$$

Rather than disassociating the CO_2 directly, H_2 can reduce CO_2 to CO via the reverse direction depending on the reaction conditions. The analysis of the CO_2 and H_2O dissociation thermodynamics shows that the WGSR is favored in the forward direction if the temperature is less than about 827°C. Above that value the WGSR is favored in the reverse direction [5].

The decomposition of a H_2O molecule is given by the following reaction [6]:

$$H_2O \rightarrow H_2 + \frac{1}{2}O_2, \Delta H = 2.6\,\text{eV/molecule} \tag{3}$$

Traditionally, in order to characterize the process efficiency, two main parameters reflecting the energy efficiency and conversion efficiency are used: conversion efficiency and energy efficiency. By definition [4], the energy efficiency η of dissociation process is given by

$$\eta = \chi \frac{\Delta H}{\text{SEI}} \tag{4}$$

where ΔH is the dissociation enthalpy of the global reaction [Eq. (1)], that is, 2.9 eV/molecule in the case of CO_2, χ is the CO_2 conversion efficiency [Eq. (5)], and SEI is the specific energy input per molecule (in eV).

The conversion efficiency of CO_2 is defined based on the following ratio:

$$\chi = \frac{\text{moles of } CO_2 \text{ converted}}{\text{moles of } CO_2 \text{ supplied}} \tag{5}$$

In our case, χ is calculated by comparing the gas chromatography (GC) CO_2 peak area without and with the presence of plasma discharge, as described in Ref. [15]. The specific energy input per molecule, SEI, is given by the ratio of the discharge power (P) to the gas flow rate (F) through the discharge volume and it can be expressed in eV per molecule.

$$\text{SEI} = \frac{P}{F} \tag{6}$$

3. Experimental part

3.1. The microwave discharge reactor

Figure 1 shows a schematic diagram of the surface-wave microwave set-up used in this work. The discharge was sustained in a quartz tube (14 mm in diameter and 31 cm in length) by an electromagnetic wave with a filling frequency of 915 MHz. The quartz tube was additionally cooled by 5°C oil. In order to minimize the reflected microwave power, the impedance of the waveguide was automatically adjusted by a three-stub tuning system. The reflected power measured for each condition was always below the detection limit of the measuring probe and thus considered negligible. The CO_2 or the other gases (Ar, O_2, H_2, or H_2O) used in our study are injected from the top of the system. The gas flow rate was regulated by electronic mass flow controllers ranging between 0 and 6 standard liter per minute (slm). The water vapor was generated in an Omicron technologies vaporization system producing a vapor flow rate between 0 and 3 slm. The obtained discharge pressure was ranging from 30 to 60 Torr. A reactor containing the catalyst was placed at the end of the plasma quartz tube, about 2 cm below the end of the tube. The sine microwave waveform (at 915 MHz) is modulated in square pulses using a dedicated power supply. Accordingly, the kHz range frequency is related to the

http://dx.doi.org/10.5772/67874

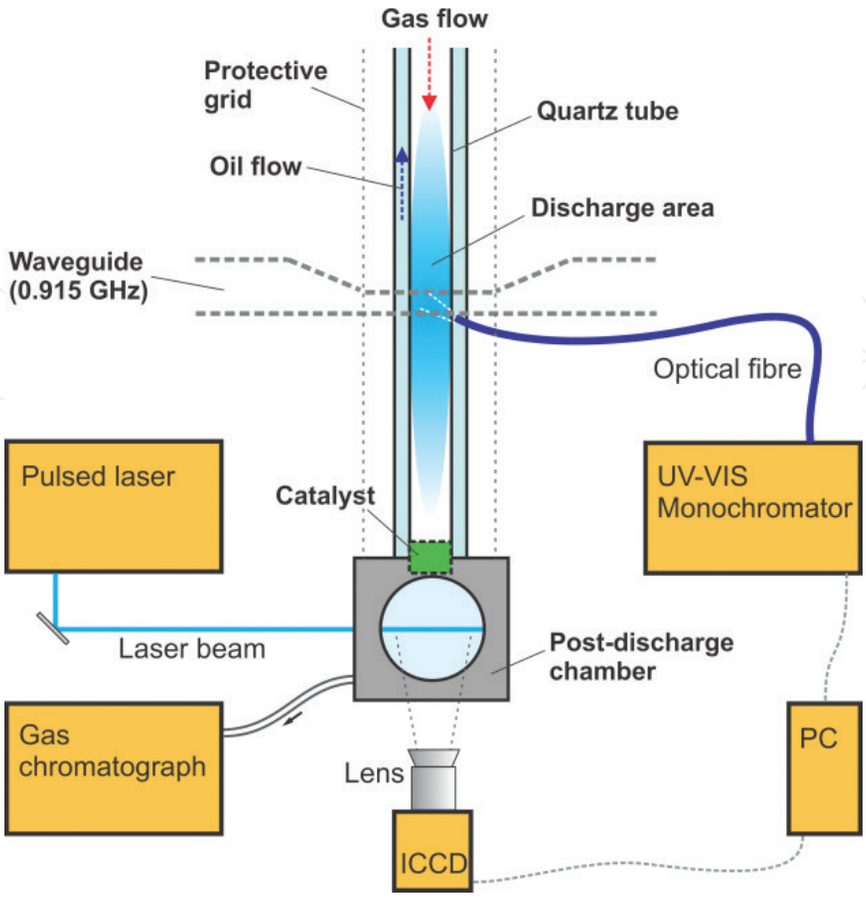

Figure 1. Schematic representation of surface-wave microwave set-up with the discharge diagnostic facilities used in this work.

modulation frequency, on top of the base frequency. In the present study, a 50% duty cycle was used: a pulse duration of 300 μs and a period of 600 μs (pulse frequency = 1.67 kHz). A more detailed description of the microwave set-up can be found elsewhere [15, 19, 32].

3.2. Characterization of plasma and dissociation products

The composition of the postdischarge was analyzed by a Bruker-450 gas chromatograph (GC) system equipped with a carbon molecular sieve column and a molecular sieve 5A column in series and connected to a thermal conductivity detector (TCD). Argon was used as a carrier gas in order to facilitate detection of H_2. CO_2, CO, H_2, and O_2 were successfully detected by GC. No hydrocarbons were detected by this current system. The microwave discharge was also characterized by optical emission spectroscopy (OES), which is a useful technique to study the large variety of chemical processes in plasma. The light emission from diatomic molecules is generally represented by a set of ro-vibrational emission bands in the studied spectral range (~300–800 nm) [33]. The vibrational populations, gas temperature, densities of the various particles and radicals, vibrational temperature, and molecular dissociation degree can be obtained through the analysis of these emission bands (as well as the atomic emission lines). The corresponding experimental data is given in the previous Chapter and also can be found elsewhere [17, 18]. The present Chapter is mainly dedicated to the effects of plasma catalysis.

3.3. Catalyst preparation

In the present work, we consider two different types of the catalyst treatment: conventional calcination and plasma treatment. Pellets (6 mm diameter and 1 mm thick) made from pure anatase powder (Sigma-Aldrich) were used as a catalyst support. We use plasma calcination as a replacement of the conventional calcination in the plasma-treatment process. Three types of catalyst were prepared by plasma processing and are denoted in this work as: NiO/TiO_2 (O_2), NiO/TiO_2 (Ar), and NiO/TiO_2 (CO_2) which corresponds to the catalysts pretreated with pure O_2 plasma, pure Ar plasma, and pure CO_2 plasma, respectively. The catalysts prepared by conventional calcination are referred to as, NiO/TiO_2 (Air-C), NiO/TiO_2 (Ar-C), for calcination in air and argon, respectively. A catalyst (NiO/TiO_2 (Ar-P)) was also studied with an Ar plasma for a longer time (similar to conventional calcination). The summary of the preparation conditions and Brunauer-Emmett-Teller (BET) surface areas is given in **Table 1**. More details about these two catalysts and the preparation can be found in the corresponding literature studies [15, 21].

3.4. Catalyst characterization techniques

The surface area of the catalyst was determined by nitrogen adsorption at a temperature of 77 K using BET analysis. At the same time, the analysis of the catalyst crystalline structure was conducted using X-ray diffraction (XRD) on the catalyst powder (Bruker advanced X-ray diffractometer (40 kV, 40 mA) with a Cu Kα (0.154 nm) at a scanning rate of 2°/min from 20 to 90°). TEM (transmission electron microscopy) (Philips CM 200) images were used to characterize the morphology and crystalline size. The Raman spectra were collected using a Bruker spectrometer equipped with a 532-nm argon ion laser as the excitation source (the laser power was 2 mW). The spectrum range was from 40 to 1000 cm^{-1} and the spectral resolution was 0.5 cm^{-1}. Raman spectrometry was also used to detect the presence of defects in the crystal lattice. Ultra violet -to- visible (UV-VIS) diffuse reflectance spectra were obtained by a Cary spectrophotometer using $BaSO_4$ as a background at a resolution of 1 cm^{-1}. It was used

Catalysts	Description	BET surface area (m^2/g)
TiO_2	Catalyst support (pure anatase)	12
TiO_2 (Ar)	Ar plasma treated for 40 minutes	12
NiO/TiO_2 (O_2)	O_2 plasma treated for 40 minutes	15
NiO/TiO_2 (CO_2)	CO_2 plasma treated for 40 minutes	19
NiO/TiO_2 (Ar)	Ar plasma treated for 40 minutes	19
NiO/TiO_2 (Air-C)	Conventional calcination in air for 2 hours	18
NiO/TiO_2 (Ar-C)	Conventional calcination in Ar for 2 hours	17
NiO/TiO_2 (Ar-P)	Ar plasma treated for 2 hours	19

Table 1. Summary of various catalysts and pure TiO_2 applied for plasma-assisted catalytic conversion of CO_2.

http://dx.doi.org/10.5772/67874

for measurements of the bandgap energy and the absorbance of ultraviolet light as a function of the wavelength.

4. Plasma-assisted catalytic conversion of CO_2

4.1. The influence of catalyst preparation method

In the field of catalysis, the nature of the catalyst in terms of its physical structure and chemical properties is a key factor for its effectiveness in a particular process. The activity of the adsorption sites provided by the catalyst determines the mechanisms that provide the lower energy reactive pathways [28]. The formation of these adsorption sites could be sensitively affected by catalyst preparation conditions, and the understanding of the chemical basis for this is essential. The nonthermal plasma, having highly energetic electrons and chemically reactive species (e.g., free radicals, excited atoms, ions, and molecules), may modify surface properties of the catalyst, enhance the dispersion of the supported metals, and even create disorder in their crystallite structure, depending on the nature of the gas phase, and the experimental treatments conditions. In this work, in order to study the relationship between the catalyst preparation method (its structure, morphology, and defect) and its efficiency in the CO_2 conversion, two different catalyst preparation methods, namely the conventional calcination and plasma treatment, were considered. Comparison of CO_2 conversion and energy efficiencies in the microwave discharge with and without catalysts as well as the effect of different preparation methods are investigated and presented in **Figure 2**. Thermally calcinated

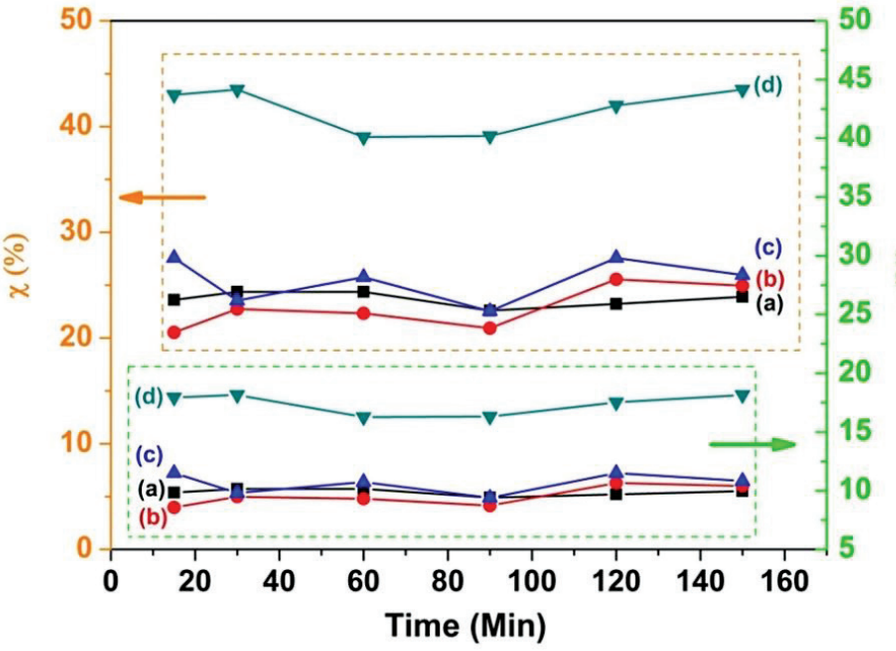

Figure 2. CO_2 conversion and energy efficiencies are shown for the NiO/TiO_2 catalysts prepared by different methods (conventional calcination vs Ar plasma treatment). (a) Plasma only, (b) NiO/TiO_2 (Air-C), (c) NiO/TiO_2(Ar-C), (d) NiO/TiO_2 (Ar-P). Flow rate = 2 slm; pressure = 30 Torr; SEI = 6.95 eV/molecule. pulse frequency = 1.67 kHz.

catalysts (NiO/TiO_2 (Air-C) and NiO/TiO_2 (Ar-C)) affect the CO_2 conversion rather insignificantly (in comparison with the plasma-only-assisted CO_2 dissociation). On the other hand, it is clear that the presence of plasma-activated catalyst (NiO/TiO_2(Ar-P) significantly enhances the CO_2 conversion and energy efficiencies compare to the plasma-only-assisted decomposition. The CO_2 conversion and energy efficiencies increase from 23 to 43% and 10 to 18%, respectively, compared to the plasma only case. For better understanding of the influence of the different preparation methods on chemical and physical properties of the catalysts, the chemical composition and morphology of the catalysts were studied by XRD, BET analysis, TEM, and Raman spectroscopy.

The catalyst characterization based on XRD and TEM results shows that an Ar plasma treatment results in a very uniform distribution of nickel oxide on the TiO_2 and the possibility of a higher Ni^{2+} concentration into the TiO_2 lattice. Raman spectroscopy was used in order to access the phase constitution and lattice defects of the catalyst support (TiO_2). All observed Raman peaks correspond to the characteristic Raman modes of the anatase TiO_2 structure [34, 35] (**Figure 3**). The peak shift in Raman spectra indicates that the vibrations of the TiO_2 lattice are considerably affected by the presence of Ni ions. The largest shift and broadening occur for the Ar plasma-treated catalyst (NiO/TiO_2 (Ar-P)), as shown in **Figure 3**. The E_g peaks are associated with the symmetric stretching vibration mode of O-Ti-O in TiO_2. This mode is very sensitive to local oxygen coordination surrounding the metal ions. According to a previous detailed analysis of Raman spectra of TiO_2 and doped-TiO_2 samples [15], the broadening and shifting of the main bands can be attributed to the presence of oxygen vacancies. These results indicate that plasma treatment can induce higher density of oxygen vacancies compared to the conventional calcination. To get a valuable insight into the catalyst activation process, a two-dimensional model of Ar plasma was developed in the modeling framework PLASIMO [36–38]. The results from the simulation imply the effective catalyst activation by the Ar metastable species (4s $1s_5$ and 4s $1s_3$ states) at the catalyst chamber region [21]. The complex environment encountered

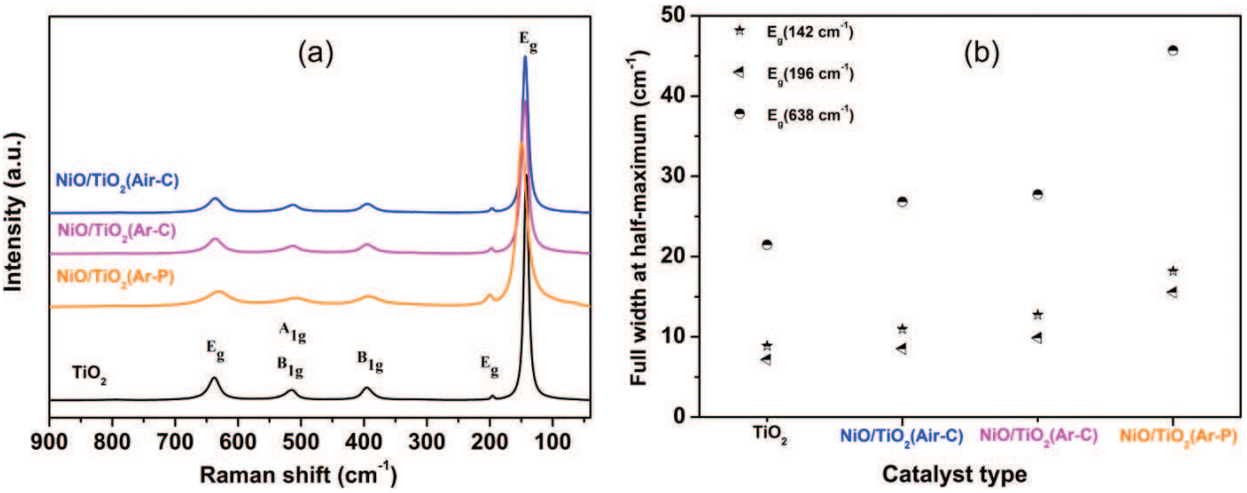

Figure 3. (a) Raman spectra of conventional calcined and plasma-treated catalysts and pure TiO_2; (b) full-width at half-maximum (FWHM) in E_g modes in the different catalysts and TiO_2 support.

http://dx.doi.org/10.5772/67874

in plasma could lead to the unusual catalyst structure, formation of smaller particles, better dispersion, and stronger interaction between the catalyst and the support.

4.2. The influence of plasma gas for catalyst activation

As mentioned above, plasma plays an important role in tailoring the properties of a catalyst by the selective doping of a material with heteroatoms and its subsequent modification of the bandgap of a material which can affect both activity and selectivity [28]. However, modifications of the catalyst depend on the nature of plasma gas and experimental treatment conditions. The influence of preactivation of the catalyst using three different gases, namely O_2, Ar, or CO_2, on the CO_2 conversion and energy efficiencies as well as on the chemical and physical properties is studied in this section. The CO_2 conversion and energy efficiencies are not altered significantly in the presence of TiO_2 (Ar) support (without doping agent) compared to the plasma-only CO_2 decomposition case, as shown in **Figure 4**. The presence of NiO/TiO_2 (Ar) significantly increases the CO_2 conversion efficiency and energy efficiency almost twice from 23 to 42% and 9.6 to 17.5%, respectively, comparing with the plasma-only experiment results. However, the CO_2 conversion and energy efficiencies were not significantly affected when NiO/TiO_2 (O_2) and NiO/TiO_2 (CO_2) catalysts are used. To understand this effect, the analysis of different catalysts and supports was undertaken by XRD, BET, Raman spectroscopy, and UV-VIS spectroscopy. Similar crystallite sizes (around 46 nm) were observed for pure TiO_2 support, TiO_2 (Ar) and NiO/TiO_2 catalysts prepared by plasma [15]. On the other hand, the lattice constant c increases slightly with the addition of NiO and the largest increase

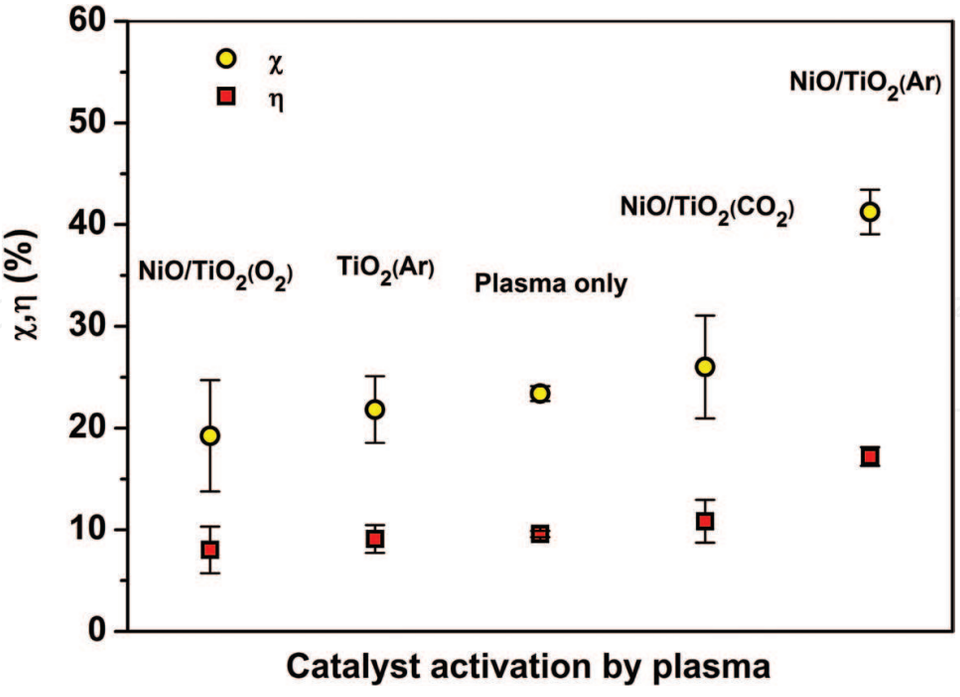

Figure 4. CO_2 conversion and energy efficiencies are shown for the NiO/TiO_2 catalysts prepared by plasma treatment with different gases (O_2, Ar, CO_2). Flow rate = 2 slm; pressure = 30 Torr; SEI = 6.95 eV/molecule. Pulse frequency = 1.67 kHz. Reprinted with permission from Ref. [15]. Copyright 2016 Elsevier.

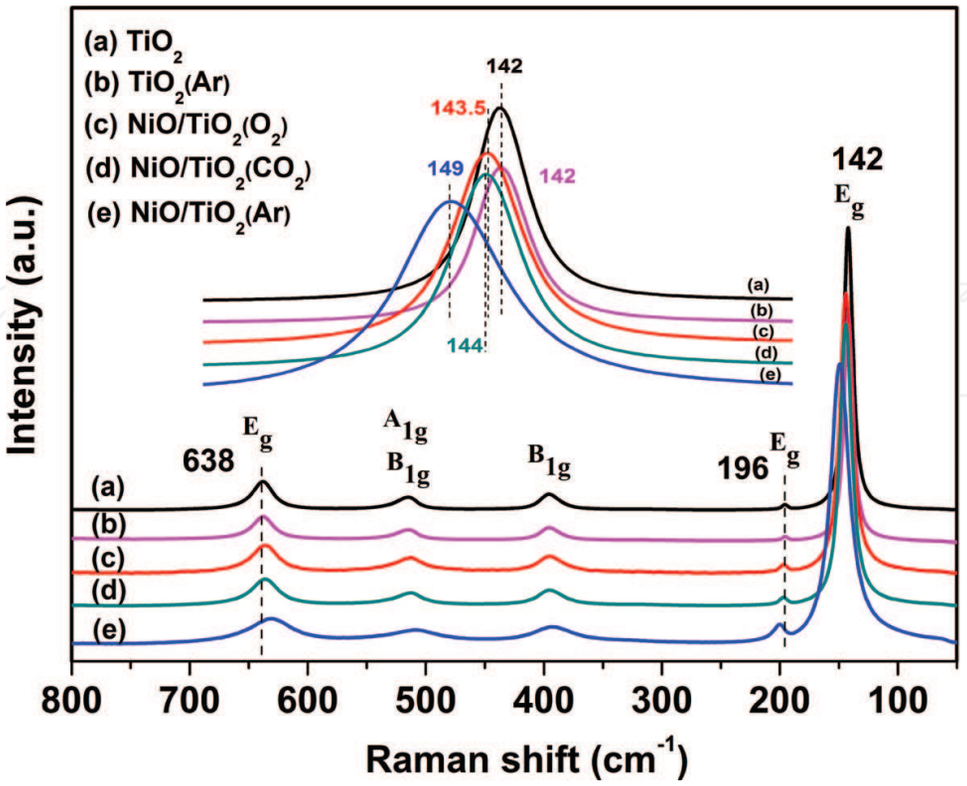

Figure 5. Raman spectra of TiO_2-supported NiO catalysts, TiO_2 (Ar), and pure TiO_2 support. The enlarged view of the intense E_g peak is shown in the inset. Reprinted with permission from Ref. [15]. Copyright 2016 Elsevier.

is observed for NiO/TiO_2 (Ar) catalyst based on the comparison of the lattice values for the NiO/TiO_2 catalysts with pure TiO_2. The observed TiO_2 lattice expansion might imply that a few Ni^{2+} ions are incorporated into the TiO_2 lattice (the ionic radius of Ni^{2+} (0.83 Å) is larger than that of Ti^{4+} (0.75Å) [39]). As we have discussed in Section 4.1, the oxygen vacancies are probably mainly responsible for the blue and red shifts as well as for widening of the Raman peaks corresponding to E_g modes. Together with the XRD results, we conclude the substitution of Ti^{4+} ions by Ni^{2+} distorts the TiO_2 lattice and generates oxygen vacancies to maintain charge neutrality. As it is noted from **Figure 5** that the largest shift and widening occur for the Ar plasma-treated NiO/TiO_2 catalyst. This indicates that the Ar plasma treatment leads to a higher concentration of oxygen vacancies in the presence of NiO. In order to study the doping effect on the catalyst optical properties, the bandgap energy E_{bg} was calculated based on the UV-VIS spectra [15]. The obtained bandgap energies are 2.85, 2.79, 2.60, 2.49, and 2.17 eV for pure TiO_2, TiO_2 (Ar), NiO/TiO_2 (O_2), NiO/TiO_2 (CO_2), and NiO/TiO_2 (Ar), respectively. These results are consistent with the previous findings that the increasing of oxygen vacancies results in a narrowing bandgap energy for TiO_2 [40–43]. The pure TiO_2 support and the TiO_2 support pretreated with Ar plasma were also investigated. No influence of Ar plasma pretreatment on the TiO_2 support surface area and its crystalline structure as well as on the defect formation has been found. Therefore, it proves that an important condition for the formation of oxygen vacancies by means of Ar plasma pretreatment is the presence of Ni^{2+} which leads to incorporation of the Ni^{2+} ions in the TiO_2 lattice.

http://dx.doi.org/10.5772/67874

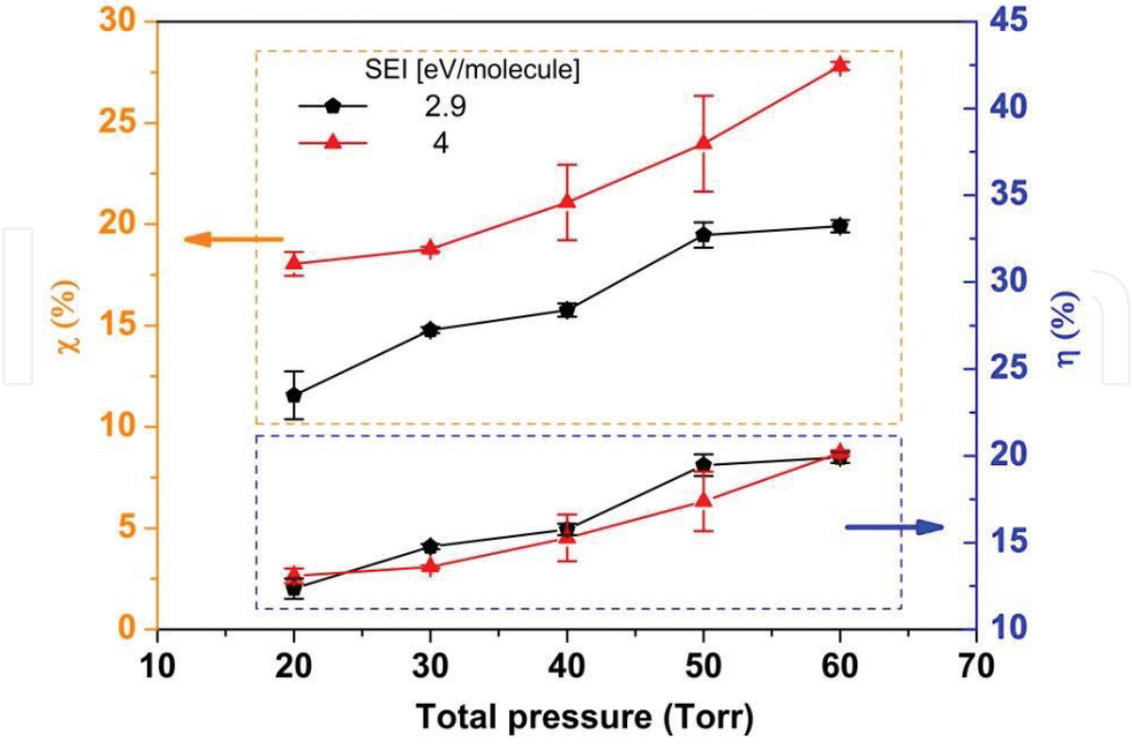

Figure 6. Evolution of the conversion efficiency and energy efficiency of CO_2 as a function of the discharge pressure at different SEI.

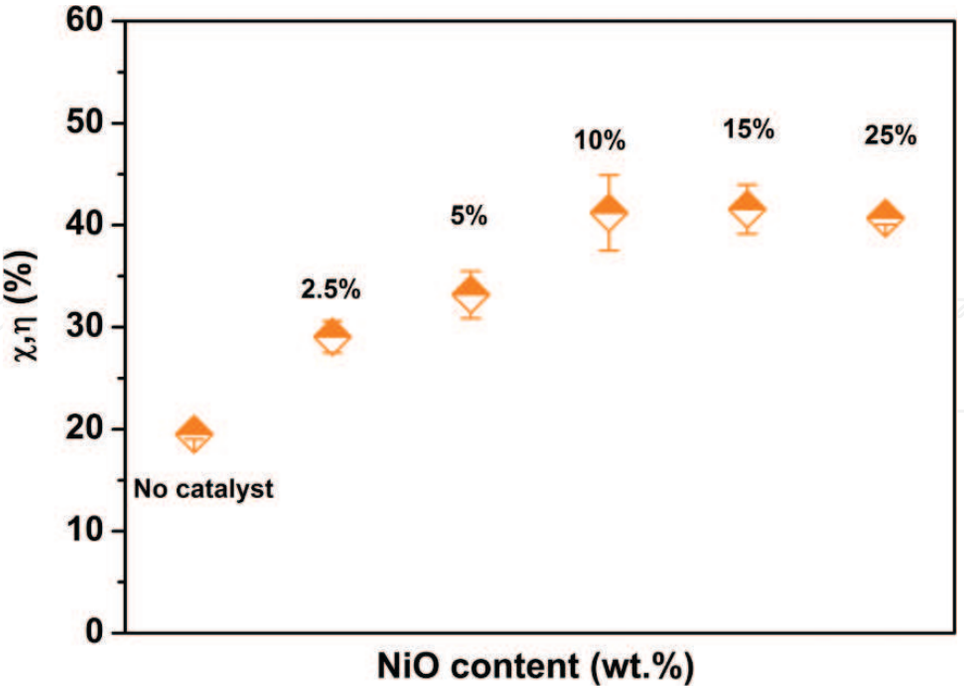

Figure 7. Dependence of the CO_2 conversion and energy efficiencies on the NiO content in the NiO/TiO_2 catalysts treated by Ar plasma. Flow rate = 5 slm; pressure = 60 Torr; SEI = 2.9 eV/molecule. Pulse frequency = 1.67 kHz.

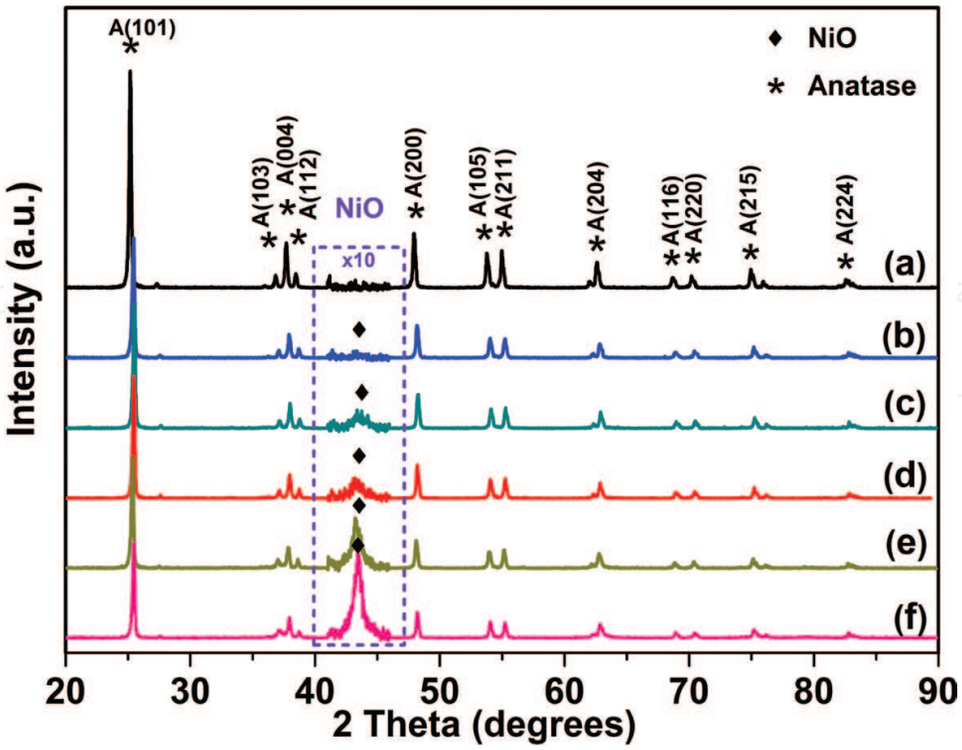

Figure 8. XRD patterns of plasma-treated catalysts with different NiO loading and pure TiO_2: (a) TiO_2, (b) 2.5 wt% NiO, (c) 5 wt% NiO, (d) 10 wt% NiO, (e) 15 wt% NiO, (f) 25 wt% NiO. The peaks, associated with the anatase phase and denoted with * in the XRD pattern of the pure TiO_2 (anatase) support, are observed with the similar intensity in all samples.

4.3. The influence of pressure and NiO content

First, the total pressure effect on the CO_2 decomposition was studied in the absence of catalyst in the range of 20–60 Torr at different SEI (**Figure 6**). As the pressure increases, our experimental data clearly show an improvement in CO_2 conversion, which is in good agreement with published results obtained in microwave plasma at low pressure [6]. These pressure-dependent results can be understood based on the increase of electron-neutral collision frequency in the plasma phase which favors the vibrational excitation of the asymmetric vibrational mode of CO_2 and leads to higher CO_2 conversion efficiency [6]. In addition, η drops when SEI increases whereas at the same time χ increases. This trade-off between χ and η has been observed in other CO_2 experiments as well [6, 10]. From this result it is clear that χ does not increase to the same extent as SEI does. The effect of nickel contents on the CO_2 conversion and energy efficiencies was investigated at 60 Torr. Increasing the nickel content from 2.5 to 10 wt% results in an increase of the CO_2 conversion and energy efficiencies up to 42% (**Figure 7**). However, at higher nickel content, there is no significant change in the conversion of CO_2. **Figure 8** shows the X-ray powder diffraction patterns of NiO/TiO_2 catalysts for different NiO contents. For nickel contents ranging from 2.5 to 10 wt%, very weak diffraction peaks were observed at $2\theta = 43.5^{o}$, corresponding to the (200) crystal planes of face-centered cubic NiO lattice. As a result of further increase of the NiO content, NiO diffraction peaks become clearly visible. This increase in the NiO content does not increase the population of

http://dx.doi.org/10.5772/67874

Ti^{4+} substituted by Ni^{2+} in the TiO_2 lattice. Further investigations are necessary to obtain a better understanding of the role of NiO.

5. Discussion

Among several factors giving significant improvements in both χ and η values, the following two groups are of special interest: the nature of plasma activation gas and NiO content on the TiO_2 surface. Compared to the plasma-only case, the CO_2 conversion and energy efficiencies were multiplied by a factor of 2.1 by selecting the appropriate catalyst preparation methods (plasma) and the NiO content. In agreement with previous study [19] on the CO_2 conversion efficiency and the corresponding relative Raman shifts of the three E_g modes observed in NiO/TiO_2 (O_2, Ar, CO_2), NiO/TiO_2 (Air-C), NiO/TiO_2 (Ar-C), NiO/TiO_2 (Ar-P), and in TiO_2 (Ar) (shown in **Figures 3** and **5**), the present results indicates that the higher activity observed on Ar plasma-treated NiO/TiO_2 catalysts could be linked to the formation of surface oxygen vacancies.

It is well known that photocatalysts can be activated through the formation of electron-hole (e^--h^+) by photoillumination of the catalyst surface. TiO_2-based catalysts are extensively studied for CO_2 photoreduction because of the adequate bandgap of TiO_2 (3.2 eV for anatase phase). Liu et al. [44] have shown that the mechanism of activation and subsequent reduction of CO_2 involves the participation of protons and electron transfer. However, with a pure TiO_2 (Ar) support, no difference in the CO_2 conversion efficiency compared to plasma only case was found, as shown in **Figure 8**. Hence, the observed improvements in our work could not be explained by the possible photoreduction of CO_2 induced by the plasma radiation.

Nowadays, the fabrication of oxygen-deficient surfaces has increasing interest, which is an important strategy for improving the photocatalytic CO_2 dissociation [44–46]. Oxygen vacancy (Vo) has been considered as the active site for the adsorption and activation of CO_2. The electron attachment to a CO_2 molecule adsorbed by an oxygen vacancy leads to the formation of a transient negative ion CO_2^- that decomposes to give CO and fill the Vo with an oxygen atom between a Ni^{2+} and Ti^{4+} ions (the oxygen atom is O_{br}) [15]. The threshold energy for this one-electron process is found to be 1.4 eV [44, 47]. The dissociative electron attachement (DEA) of CO_2 observed on the catalytic surface can occur also in the gas phase [6]. However, the maximum value of the DEA cross-section is low ($\sim 10^{-22}$ m^2) and the threshold energy of 5–10 eV [6] is high compared to the threshold energy of 1.4 eV [47] for the DEA at the catalyst surface. So, the DEA process for CO_2 occurs more easily for adsorbed CO_2 on the TiO_2 defective surface than for CO_2 in the gas phase. As the activity of our catalyst remains constant over time, a regeneration of Vo is necessary [15].

A study of CO_2 conversion efficiency in different gas mixtures in the presence of NiO/TiO_2 (Ar-P) has also been investigated [19, 21]. It was found that the CO_2 conversion efficiency was also enhanced independently of the mixture when NiO/TiO_2 (Ar-P) is used. A synergy between the catalyst and plasma is clearly demonstrated. The CO_2 conversion and energy efficiencies in 90% CO_2–10% H_2O increase from 30 to 52% and 12.5 to 22%, respectively,

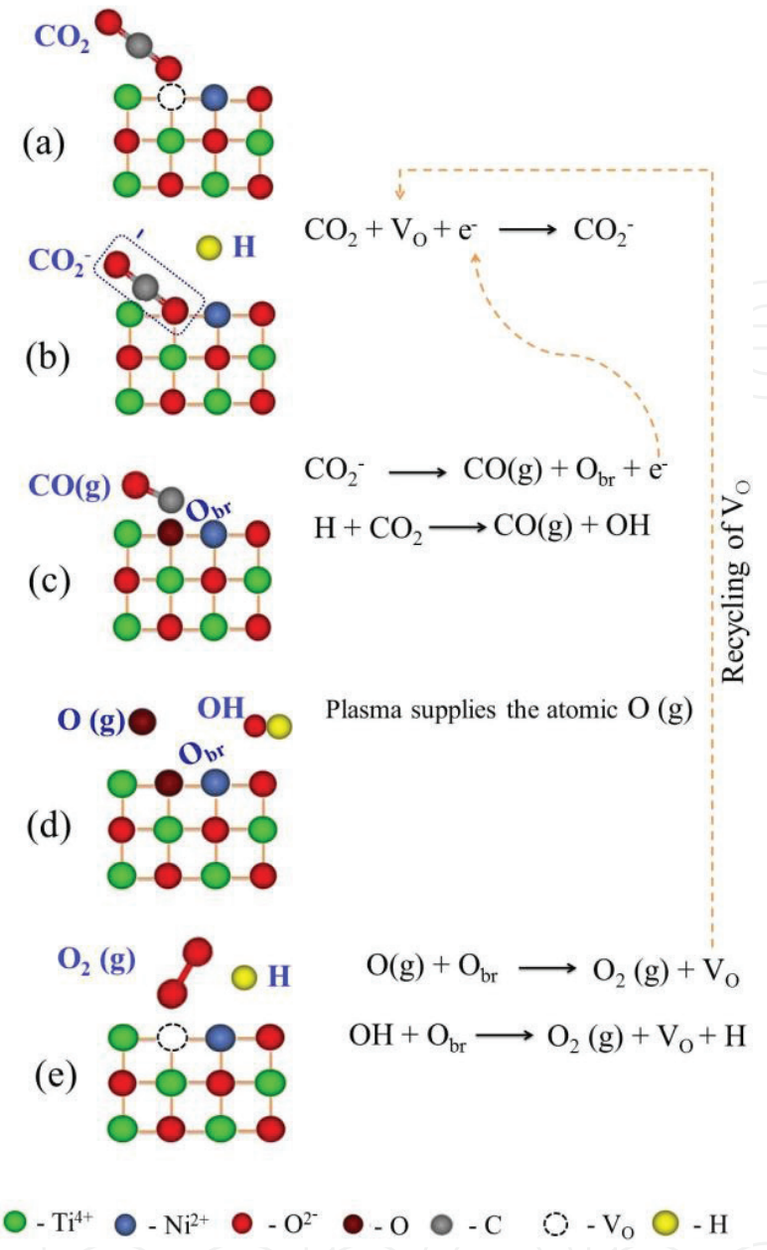

Figure 9. A tentative mechanism of plasma-catalytic CO_2 decomposition on the catalyst surface.

when the activated catalyst is combined with the plasma. We found previously that oxygen vacancies enhanced the CO_2 conversion in the plasma-catalytic dissociation of pure CO_2 [15]. The electrons supplied by the plasma enhance the dissociative attachment of CO_2 on the oxygen-deficient catalyst surface. We suggest that the following processes can be distinguished on the catalyst surface in the plasma-catalytic CO_2/H_2O conversion (**Figure 9**). CO_2 could be reduced to CO via reaction with H radical or direct dissociation by healing the oxygen vacancy sites [1, 48, 49]. The active species OH and adsorbed oxygen atom react with each other to form atomic hydrogen and O_2, resulting in the regeneration of oxygen vacancy. The oxygen vacancy can also be regenerated via the recombination on the surface of a bridging oxygen atom with a gaseous oxygen atom [15, 50, 51]. The presence of atomic

http://dx.doi.org/10.5772/67874

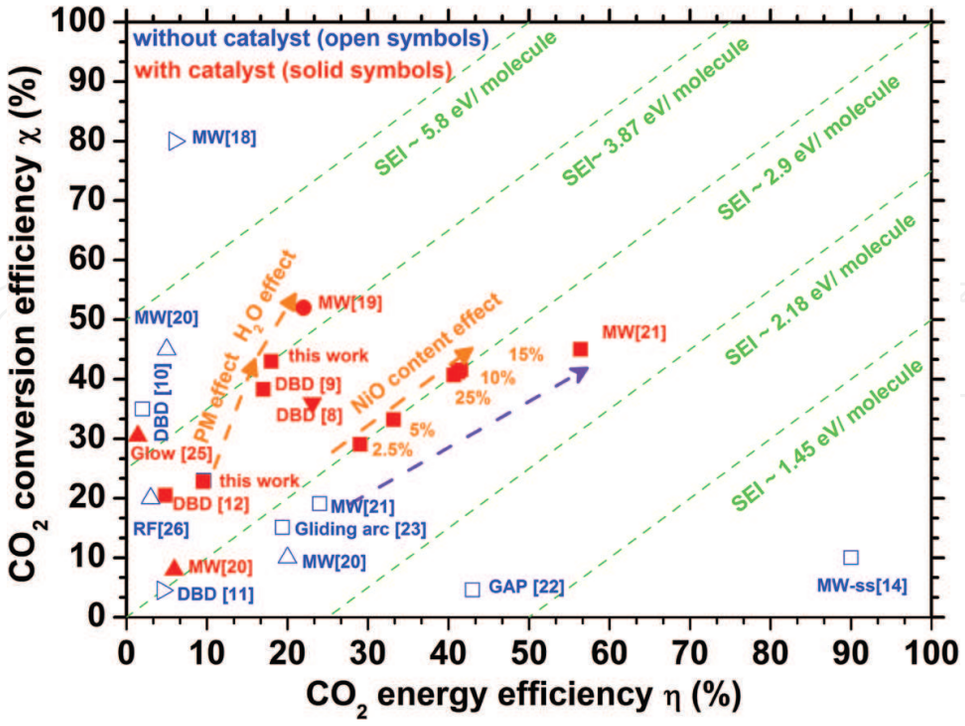

Figure 10. Comparison of the conversion and energy efficiencies for CO2 with different types of non-thermal plasmas: □, ■ - Pure CO2; Δ, ▲ - CO2-Ar mixture; ● - CO2-H2O mixture; ▼ CO2-H2O -Ar mixture; ▷-CO2-N2 mixture. PM stands for Preparation Method, MW-ss stands for a Microwave discharge with supersonic gas flow. The SEI values are given for reference.

O peaks and water dissociation product (OH and H) peaks in the emission spectrum of CO_2/H_2O microwave discharge was detected and reported in our previous study [17]. The plasma supplies energy to the catalyst surface and thus additionally enhances the recombination process. The regeneration of oxygen vacancies can be confirmed by our experimental results [19, 21]. The CO_2 conversion and energy efficiencies remain more or less constant over time, at least for 150 minutes of continuous operation. Hence, a synergistic effect between the plasma and the NiO/TiO_2(Ar-P) catalyst leads to significantly improved CO_2 conversion and energy efficiencies, which can be attributed to the dominant surface reactions driven by the plasma.

A two-dimensional χ-η chart compares the energy efficiency for CO_2 conversion using different types of nonthermal plasmas (**Figure 10**). The influence of the NiO content, as well as of the other effects studied (such as H_2O effect) in this and previous work [19, 21] is clearly visible. Selected results on CO_2 conversion taken from the literature are given for comparison. The data points corresponding to our study look very promising. The highest energy efficiency of about 90% was reported by Asisov et al. in microwave plasma in supersonic flow [14]. The corresponding CO_2 conversion was only about 10%, which is significantly lower than that (42%) obtained in this work for pure CO_2 decomposition with a catalyst. The highest reported conversion efficiency was about 80% while the energy efficiency was less than 6% [18]. A balance between CO_2 conversion and energy efficiencies in the plasma processing of CO_2 is especially important for the development of an efficient and cost-effective process. The combination

of the microwave plasma and the Ar plasma-treated NiO/TiO_2 catalyst leads to significant enhancement in the CO_2 conversion and energy efficiencies of the plasma process, as well as the balance between them.

6. Conclusions

This work critically summarizes the effects of various plasma operating conditions and catalyst preparation methods on the CO_2 conversion and its energy efficiency in a surface-wave sustained microwave discharge. As a result, one can conclude that the catalyst preparation method has a significant impact on the chemical and physical properties of the catalysts, which in turn strongly influence CO_2 conversion and energy efficiencies. Ar plasma treatment is supposed to result in a higher density of oxygen vacancies and a very favorable distribution of nickel oxide on the TiO_2 surface comparing with the classical calcination in air or in argon.

The oxygen vacancies are the key factor explaining the catalytic activities in CO_2 decomposition. These vacancies are stabilized by the presence of Ni^{2+} ions in the anatase lattice. The plasma pretreatment allows to both create oxygen vacancies, and to incorporate the nickel into the TiO_2 lattice to stabilize these vacancies. The dissociative electron attachment of CO_2 at the catalyst surface enhanced by the oxygen vacancies and plasma electrons can explain the observed increase of CO_2 conversion as well as the energy efficiency. A mechanism is proposed that explains the observed plasma-catalyst synergy, which has led to improved CO_2 conversion and energy efficiencies.

At the same time, there is still a room for further improvement of the CO_2 conversion and energy efficiencies through the optimization of the plasma parameters (e.g., high pressure and high flow rate) and the modification of catalysts (e.g., loading different metal nanoparticles on TiO_2). In addition, it is very promising to explore the possibility of H_2O-CO_2 as an alternative system to conversion of carbon dioxide to value-added compounds, such as syngas, methanol, and formic acid. We expect that the results presented in this study will provide useful insights into the plasma-assisted CO_2 conversion in the presence or absence of catalysts, which may be used for greenhouse gas conversion in industry.

Acknowledgements

The authors acknowledge the financial support from the network on Physical Chemistry of Plasma Surface Interactions-Interuniversity Attraction Poles phase VII project (http://psi-iap7.ulb.ac.be/), supported by the Belgian Federal Office for Science Policy (BELSPO). G. Chen is grateful to Violeta Georgieva, Tiriana Segato, Patrizio Madau, and Löic Malet (Université Libre de Bruxelles) and to Sylvain Deprez (Materia Nova Research Center) for their valuable help in catalyst characterization and discussion. N. Britun and T. Godfroid acknowledge the support of the "REFORGAS GreenWin" project (grant No. 7267).

http://dx.doi.org/10.5772/67874

Author details

Guoxing Chen[1,2]*, Nikolay Britun[2], Thomas Godfroid[3], Marie-Paule Delplancke-Ogletree[1] and Rony Snyders[2,3]

*Address all correspondence to: guoxchen@ulb.ac.be

1 4MAT, Free University of Brussels, Belgium

2 Chemistry of Plasma Surface Interactions, University of Mons, Belgium

3 "Materia Nova" Research Center, Belgium

References

[1] Rayne, S. Carbon Dioxide Splitting: A Summary of the Peer-Reviewed Scientific Literature. Available from Nature Precedings, 2008. DOI:10.1038/npre.2008.1741.1.

[2] Traynor A J, Jensen R J. Ind. Eng. Chem. Res. 2002; **41:** 1935–1939.

[3] Hu B, Guild C, Suib S L. J. CO_2 Util. 2013; **1**: 18–27.

[4] Stechel E B, Miller J E. J. CO_2 Util. 2013; **1**: 28–36.

[5] Graves C, Ebbesen S D, Mogensen M, Lackner K S. Renew. Sust. Energ. Rev. 2011; **15**: 1–23.

[6] Fridman A. Plasma Chemistry. Cambridge University Press, New York, 2008.

[7] Zou J, Liu C. Utilization of Carbon Dioxide Through Nonthermal Plasma Approaches. Wiley-VCH Press, ISBN: 978-3-527-32475-0, 2010. DOI: 10.1002/9783527629916.ch10.

[8] Mahammadunnisa S, Reddy L, Ray D, Subrahmanyam C, Whitehead J C. Int. J. Greenh. Gas Con. 2013; **16**: 361–363.

[9] Mei D, Zhu X, Wu C, Ashford B, Williams P P, Tu X. Appl. Catal., B. 2016; **182**: 525–532.

[10] Aerts R, Somers W, Bogaerts A. Chem Sus Chem. 2015; **8**: 702–716.

[11] Snoeckx R, Heijkers S, Wesenbeeck K Van, Lenaerts S, Bogaerts A, Energy Environ Sci., 2016; **9**: 999–1011.

[12] Yu Q, Kong M, Liu T, Fei J, Zheng X. Plasma Chem Plasma Process. 2012; **32**: 153.

[13] Ozkan A, Dufour T, Bogaerts A, Reniers F. Plasma Sources Sci. Technol. 2016; **25(4)**: 045016.

[14] Asisov R I, Givotov V K, Krasheninnikov E G, Potapkin B V, Rusanov V D, Fridman A. Sov. Phys., Doklady 1983; **271**: 94.

[15] Chen G, Georgieva V, Godfroid T, Snyders R, Delplancke-Ogletree M P. Appl. Catal. B: Environ. 2016; **190**: 115–124.

[16] Van Rooij G J, van den Bekerom D C M, Den Harder N, Minea T, Berden G, Bongers W A, Engeln R, Graswinckel M F, Zoethout E, Van de Sanden M C M. Faraday Discuss. 2015; **183**: 233–248.

[17] Chen G, Silva T, Godfroid T, Godfroid T, Britun N, Snyders R, Delplancke-Ogletree M P, Int. J. Hydrogen Energy. 2016; **40**: 3789–3796.

[18] Silva T, Britun N, Godfroid T, Snyders R. Plasma Sources Sci Technol. 2014; **23**: 025009.

[19] Chen G, Britun N, Godfroid T, Godfroid T, Snyders R, Delplancke-Ogletree M P. J. Phys. D: Appl. Phys. 2017; **50**: 084001.

[20] Spencer L F, Gallimore A D. Plasma Sources Sci. Techenol. 2013; **22**: 015019.

[21] Chen G, Godfroid T, Britun N, Georgieva V, Delplancke-Ogletree M P, Snyders R. Appl. Catal. B: Environ. 2016. *Submitted*.

[22] Nunnally T, Gutsol K, Rabinovich A, Fridman A, Gutsol G, Kemoun A. J. Phys. D: Appl. Phys. 2011; **44**: 274009

[23] Indarto A, Yang D R, Choi J W, Lee H, Song H K, J. Hazard. Mater. 2007; **146**: 309–315.

[24] Sun S R, Wang H X, Mei D H, Tu X, Bogaerts A, J. CO_2 Util. 2017; **17**: 220–234.

[25] Brock S L, Marquez M, Suib S L, Hayashi Y, Matsumoto H. J. Catal. 1998; **180**: 225–233.

[26] Spencer L F, Gallimore A D. Plasma Chem. Plasma Process. 2011; **31**: 79–89.

[27] Mikoviny T, Kocan M, Matejcik S, Mason N J, Skalny J D. J. Phys. D: Appl. Phys. 2004; **37**: 64.

[28] Chung W C, Chang M B. Renew. Sustain. Energy Rev. 2016; **62**: 13–31.

[29] Whitehead J C. J. Phys. D: Appl. Phys. 2016; **49**: 243001.

[30] Chen H L, Lee H M, Chen S H, Chao Y, Chang M B. Appl. Catal., B, 2008; **85**: 1–9.

[31] Neyts E C, Ostrikov K, Sunkara M K, Bogaerts A. Chem. Rev. 2015; **115**: 13408.

[32] Godfroid T, Dauchot J P, Hecq M, Surf. Coatings Technol. 2005; **200**: 649.

[33] Herzberg G. Molecular Spectra and Molecular Structure: Spectra of Diatomic Molecules. New York: Litton Educational Publishing, 1950.

[34] Ohsaka T, Izumi F, Fujiki Y. J. Raman Spectrosc. 1978; **7**: 321.

[35] Choudhury B, Choudhhury A. Mater. Chem. Phys. 2012; **132**: 1112–1118.

[36] Georgieva V, Berthelot A, Silva T, Kolev S, Graef W, Britun N, Chen G, Van der Mullen J, Godfroid T, Mihailova D, Dijk J V, Snyders R, Bogaerts A, Delplancke-Ogletree M P. Plasma Processes Polym. 2016, DOI:10.1002/ppap.201600185

[37] The Plasimo code website: http://plasimo.phys.tue.nl/

[38] Van Dijk J, Peerenboom K S C, Jimenez-Diaz M, Mihailova DB, Van der Mullen J J A M, J. Phys. D: Appl. Phys. 2009; **42**: 194012.

[39] Shannon R D. Acta Cryst A. 1976; **32**: 751–767.

[40] Suib S. New and Future Developments in Catalysis. Elsevier, Amsterdam, 2013.

[41] Wang Y, Zhang R, Li J,Li L, Lin S. Nanoscale Res. Lett. 2014; **9**: 46.

[42] Bharti B, Kumar S,Lee H N, Kumar R. Sci. Rep. 2016; **6**: 32355.

[43] Kamarulzaman N, Kasim M F, Rusdi R. Nanoscale Res Lett. 2015; **10**: 346.

[44] Liu L, Li Y. Aerosol. Aerosol. Air. Qual. Res. 2014; **14**: 453–469.

[45] Rasko J, Solymosi F. J. Phys. Chem. 1994; **98**: 7147–7152.

[46] Liu L, Zhao C, Li Y. J. Phys. Chem. C. 2012; **116**: 7904–7912.

[47] Lee J, Sorescu D C, Deng X, J. Am. Chem. Soc. 2011; **133**: 10066–10069.

[48] Tahir M, Tahir B, Amin N A S, Muhammad A. Energy Convers. Manag. 2016; **119**: 368–378.

[49] Liu L, Zhao H, Andino J M, Li Y. ACS Catalysis 2012; **2**: 1817–1828.

[50] Crane P J, Dickens P G, Thomas R E. Trans. Faraday Soc. 1967; **63**: 693–700.

[51] Kovalev V L, Krupnov A A, Pogosbekyan M Y, Sukhanov L P, Acta Astronautica. 2011; **68**: 686–690.

IntechOpen